# PULSE SEPARATION CHARACTERISTICS BASED ON THEIR APPROXIMATION

**Jiří Jevický[1], Filip Mravec[2], Zdeněk Matěj[2] Václav Přenosil[2]**
[1] Faculty of military Technology, University of Defence, Brno
jiri.jevicky@unob.cz
[2] Faculty of Informatics, Masaryk University, Brno
Botanická 68a, 602 00 Brno, Czech Republic
xmravec@fi.muni.cz, matej.zdenek@gmail.com, prenosil@fi.muni.cz

**Abstract:** *This article deals constructing of models to approximate the electrical impulses that occur originate in the detector of a nuclear radiation. Radiation detector detects two kinds of particles. Electrical impulses of both responses are different in the order of nanoseconds. Mathematical models of the individual particles responses let easily distinguish what kind of particles was detected. The article describes four separation methods and evaluated their effectiveness.*

**Keywords:** approximation; discrete orthogonal polynomials, 3D frequency histogram, scatter plot

## INTRODUCTION

Universal method of analyzing responses spectrometry detectors in mixed fields of fast neutrons and gamma rays is an effective tool for many applications. One is used in radiation protection, environmental protection, medicine, security, military, etc. Digital spectrometric detection can reduce the dimensions of measuring equipment, reduce its power consumption, reduce time measurements and measurements in the field. Separation of mixed energy field values by folders belonging neutrons and gamma rays are usually made on the basis of analog signal processing laboratory equipment and is therefore subject to laboratory conditions. Digital spectrometric detection allows to measure routinely *in sittu*.

## 1 SEPARATION METHODS OF THE RADIATION DETECTOR RESPONSES

All of the separation characteristics of the considered **C** pulse **f(t)** are based on an approximation of digitized pulse discrete orthogonal polynomials, ie the approximation:

$$\varphi(t) = \sum_{k=0}^{n} c_k P_k(t) \tag{1}$$

where the basic function $P_k(t)$ are orthogonal polynomials on the set of nodes, $t = 0, 1, \dots N$, with $N \geq n$ To generate a set of basic functions were used formula:

$$\begin{aligned} &P_0(t) = 1, \\ &P_1(t) = 1 - 2\frac{t}{N}, \\ &P_k(t) = \frac{2(2k-1)}{k(N-k+1)}\left(\frac{N}{2} - t\right)P_{k-1}(t) - \frac{(k-1)(N+k)}{k(n-K+1)}p_{K-2}(t), k = 2,3,\dots.n. \end{aligned} \tag{2}$$

Separation by an initial pulse of edge demonstrates excellent separation properties themselves coefficients $c_1$, $c_3$,, and $c_0$, $c_5$. Some functional expressions of these coefficients could then separation capabilities even stronger.

For the separation of pulses by pulse decay is shown that the separation capacity of the approximation coefficients is less significant. Good separation properties were detected only in the coefficient $\mathbf{c_0}$, and somewhat less good factor at $\mathbf{c_2}$.

Therefore were examined the properties of other variously defined separation characteristics of **C**, for example, assessing distance inflection points approximation $\mathbf{\Pi(t)}$, or expressions of integrals approximation.

As promising appears the following separation characteristics and methods.

### 1.1 Koeficient $c_0$ aproximace

First consider the response:

$$\mathbf{C = c_0} \qquad (3)$$

On Figure 1: is a scatter plot of the observed values of two-dimensional random variables **(C, Q)**, where **Q** is second characteristic are maxima of measured (digitized) pulses detected on a set of measured impulse values $\{\mathbf{f_0, f_1, \ldots, f_N}\}$. Illustration images are created using the "Spectrum 2" program (author Jevický) using data files "fotony.awd" and "neutrony.awd" (author Matěj, Cvachovec).

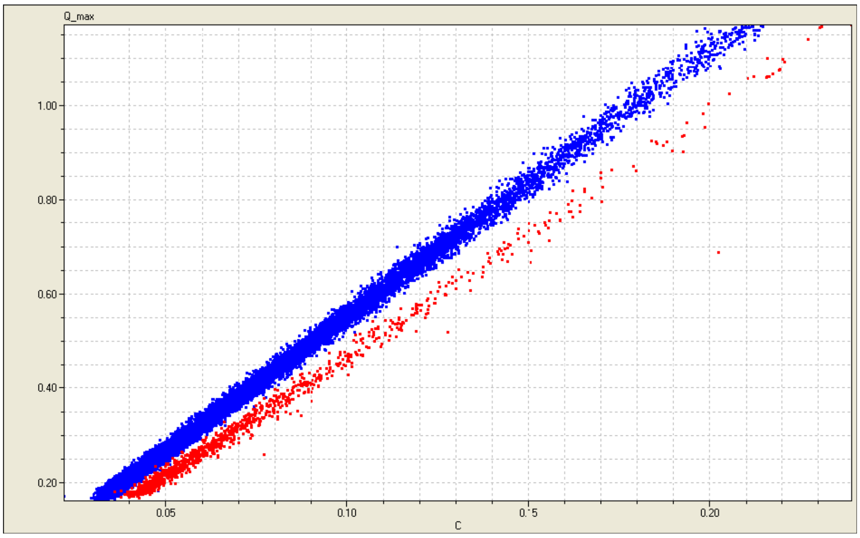


Figure 1: Scatter plot of the random variables **(C, Q)** for characteristic $\mathbf{c_0}$

Given the purpose of the separation is possible to release from the transformation equations transformation of coordinates **Q** and too the shift to a new center. New separation characteristic is possible introduce simply by following formula:

$$\mathbf{C_T = C * \cos\alpha + Q * \sin\alpha} \qquad (4)$$

where the angle $\boldsymbol{\alpha}$ (and also the values of sine and cosine) is sufficient to calculate only once in the process of calibration of the measuring device. For test data was used transformation:

**CT = C ∗ 0,01341404257942208 + Q ∗ (-0,9999100276833298).**

Scatter plot of the $\mathbf{(C_T, Q)}$ is shown on Figure 2.

For ease of separation of photons (blue dots on the charts) and neutrons (red dots) is suitable transformation of the coordinate system rotation by the angle $\boldsymbol{\alpha}$, which forms an axis regression lines $\mathbf{Q = a + b * C}$ for photons and neutrons with a vertical axis, with the center of rotation is the intersection of the regression lines.

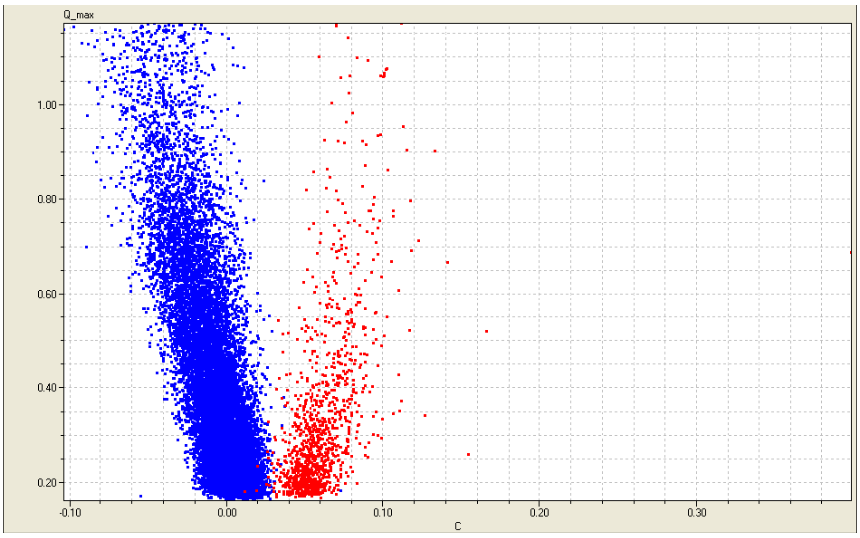


Figure 2: modified scatter plot of the variables**(C, Q)** for characteristic $\mathbf{c_0}$

According to formula (2) is $\mathbf{P_0(t) = 1}$ and hence the coefficient $\mathbf{c_0}$ of the approximation (1) is true:

$$c_0 = \frac{(f, P_0)}{(P_0, P_0)} = \frac{\sum_{i=0}^{N} f(i)P_0(i)}{\sum_{i=0}^{N} (P_0(i))^2} = \frac{1}{N+1}\sum_{i=0}^{N} f(i) \qquad (5)$$

which means that the characteristic $\mathbf{C = c_0}$ can be interpreted as the mean pulse. Since the time step in the table of pulse measured values is 1 ns pulse (and because the values of **f(t)** at the beginning and at the end of the table are virtually zero) can be the sum of the values in equation (5) taken as an approximate value of the integral of the pulse **f(t)** at interval $\langle \mathbf{0, N} \rangle$ (more precisely at the interval $\langle \mathbf{0{,}5; N + 0{,}5} \rangle$. Note, that the coefficient $\mathbf{1/(N + 1)}$ in equation (5) is constant for all pulses and therefore does not alter the properties of the actual values of the pulse sum (or integral) as separation characteristics of pulse.

### 1.2 The difference of the coefficients $c_0$ a $c_2$ of the approximation

In this case, considering the following characteristics of the pulse separation:

$$C = 10(c_0 - c_2) \qquad (6)$$

where the factor 10 is only for the purpose of scaling the axis **C** "pleasant" greater value. Scatter plot **(C, Q)** for this characteristic is on Figure 3.

Using nonlinear regression hyperbolic transformation was found next pulse characteristic:

$$C_T = \frac{C}{0{,}1 * Q - 0{,}00676} \qquad (7)$$

Scatter plot $\mathbf{(C_T, Q)}$ for the transformed separation characteristic $\mathbf{C_T}$ is on Figure 4.

### 1.3 Quotient of active edge approximations integral of the pulse and the maxima approximations of the pulse

In this method as the separation characteristics of the pulse is considered:

$$C_I = \frac{1}{\varphi_{max}} \int_{t_{\varphi\,max}}^{t_{kon}} \varphi(t)dt \qquad (8)$$

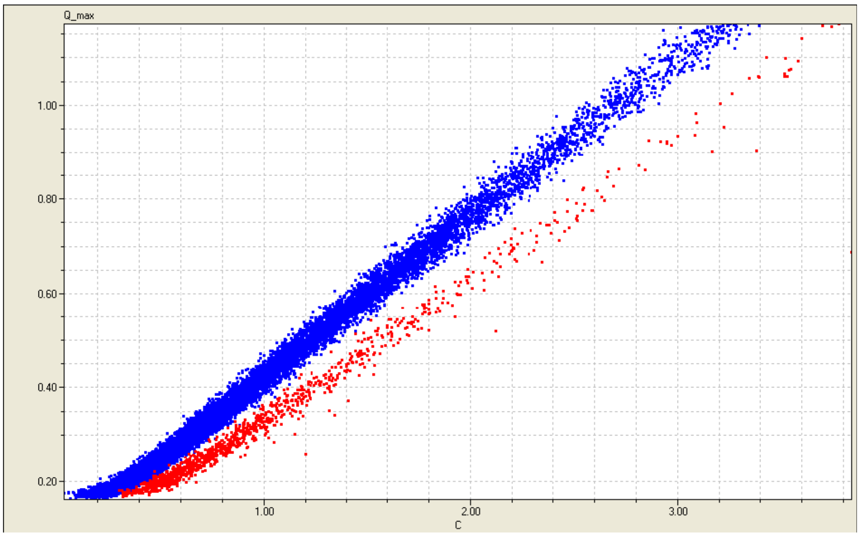


Figure 3: Scatter plot of variables **(C, Q)** for characteristic **$10(c_0-c_2)$**

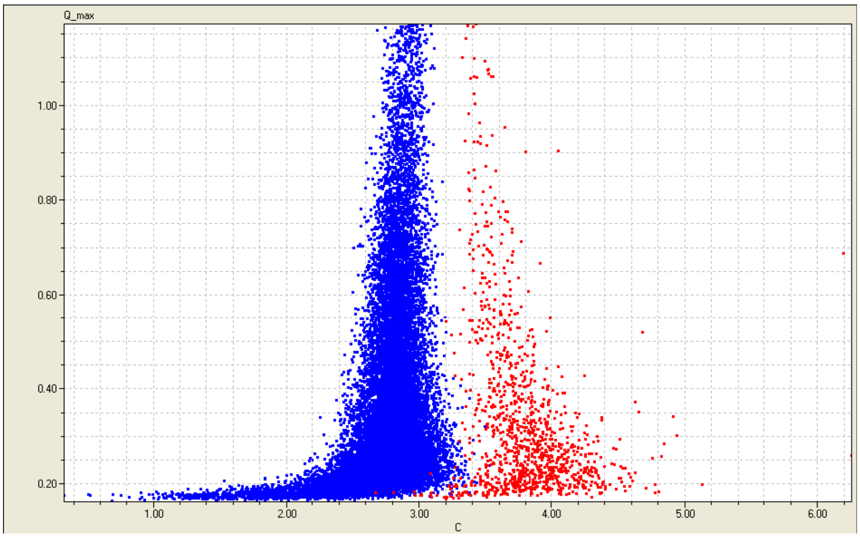


Figure 4: modified scatter plot of the variables **(C, Q)** for characteristic **$10(c_0-c_2)$**

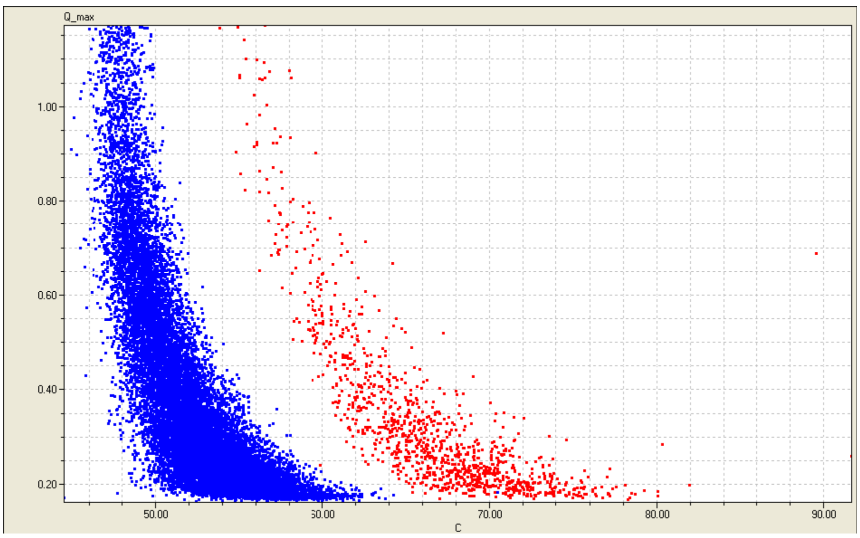


Figure 5: Scatter plot of variables **(C, Q)** for characteristic **$C_I$**

where $\varphi_{max}$ is the global maximum of the approximation $\varphi(t)$ pulse $f(t)$, $t_{\varphi max} \in \langle 0, N \rangle$ s the time at which the functions $\varphi(t)$ takes its maximum and $t_{kon} = t_{\varphi max} + d$. The length of the integration interval was chosen $d = 300$. The scatter chart $(C, Q)$ for this characteristic is shown on Figure 5.

### 1.4 Integral from approximation of the active edge pulse

In this method the separation characteristic of the pulse is:

$$C_{II} = \int_{t_{\varphi max}}^{t_{kon}} \varphi(t)dt \tag{9}$$

where $t_{\varphi max} \in \langle 0, N \rangle$ is the time at which the approximation $\varphi(t)$ pulse attains its maximum and $t_{kon} = t_{\varphi max} + d$. The length of the integration interval was chosen $d = 300$. The scatter plot of variables $(C, Q)$ for this characteristic is shown on Figure 6.

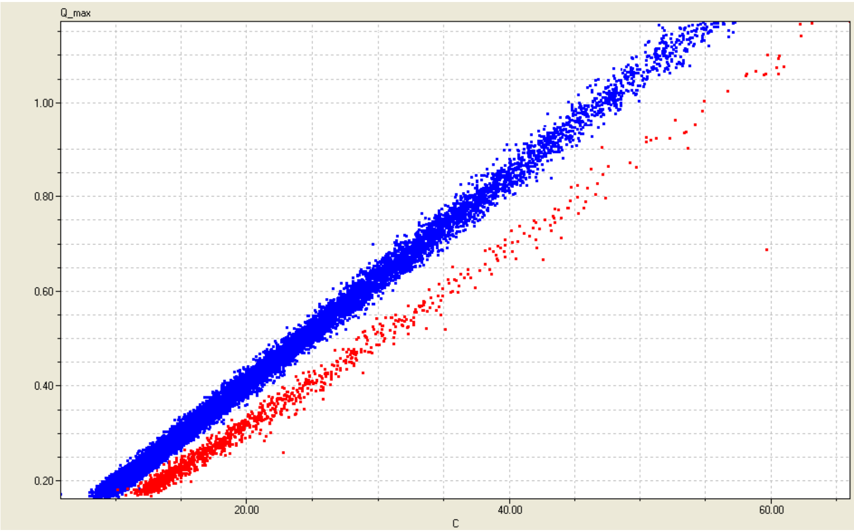


Figure 6: Scatter plot of variables $(C, Q)$ for characteristic $C_{II}$

Approximately linear dependence of random variables $C$ and $Q$ allows analogously as in the case of separation characteristic $C = c_0$ (see 1.1 ) to calculate the appropriate transformation by rotating of the coordinate system $(C, Q)$.

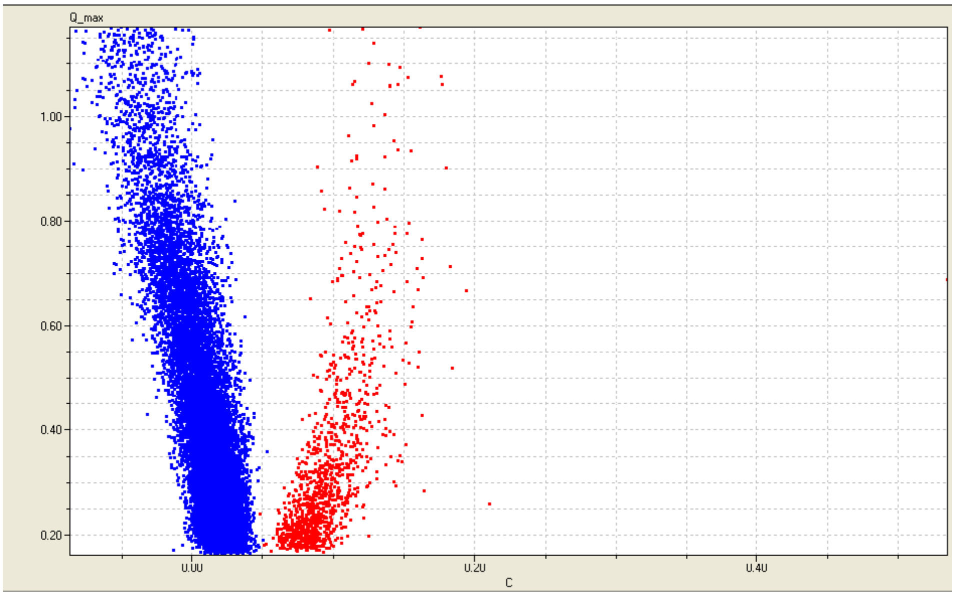


Figure 7: modified scatter plot of the variables$(C, Q)$ for characteristic $C_{II}$

The coefficients for the characteristic $\mathbf{C_{II}}$ were calculated from the following transformation formula:

$$\mathbf{C_{II} = C*0{,}02012942734552012 + Q*(-0{,}9997973825504552).}$$

Scatter plot **($C_{II}$, Q)** for the transformed separation characteristic $\mathbf{C_{II}}$ is shown on Figure 7.

## 2 OVERALL VIEW OF THE SEPARATION

The four types of separation characteristics **C** was prepared from data file "_data_10000.awd" containing records of one million pulses. After removal of deformed pulses was pair separation characteristics **(C, Q)** calculated from 985.313 pulses.

Thus obtained four statistical samples (by methods discussed in the previous chapters) were divided into a total of 1,024,512 classes.

All four dimensional frequency tables were stored in files in CSV format. The following figures are shown both frequency histograms 3D dimensional random variables **(C, Q)** and 2D scatter plots frequency tables.

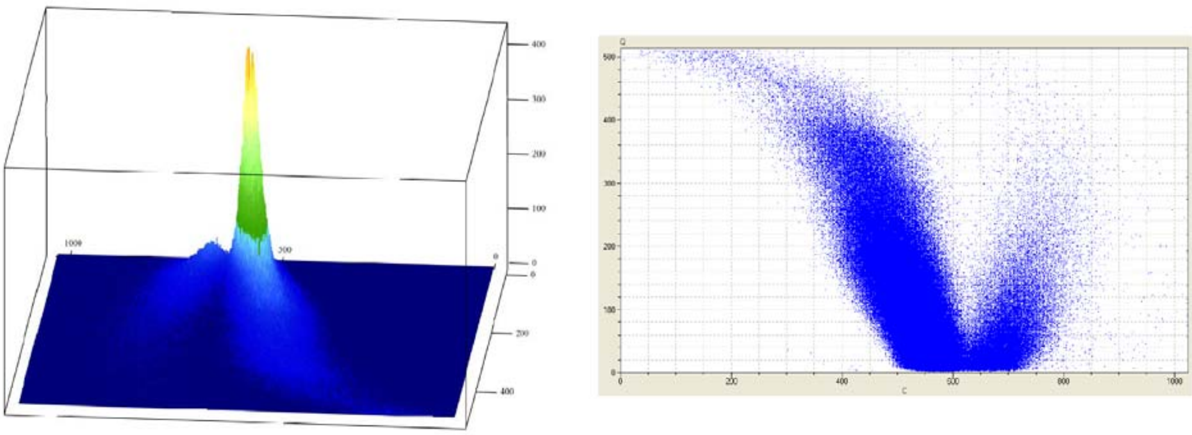

Figure 8: **C** characteristics according to the method from chapter 1.1 see file _data_10000_Aupr.csv

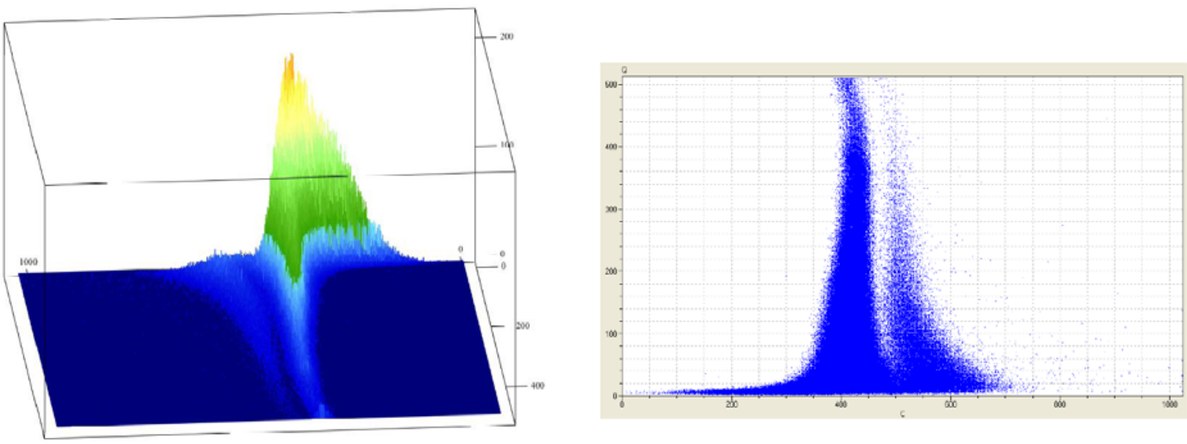

Figure 9: **C** characteristics according to the method from chapter 1.2 for file _data_10000_Bupr.csv

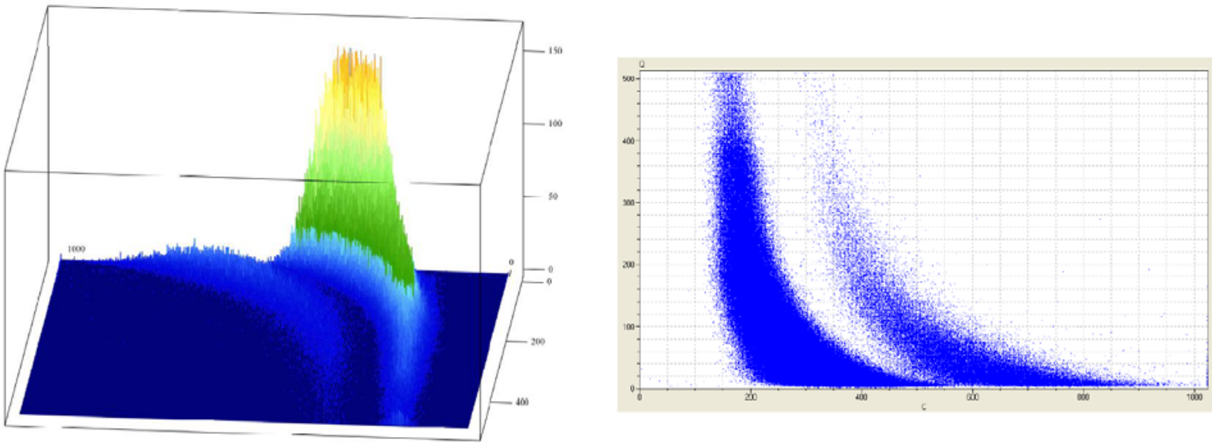

Figure 10: **C** characteristics according to the method from chapter 1.3 for file _data_10000_Cupr.csv

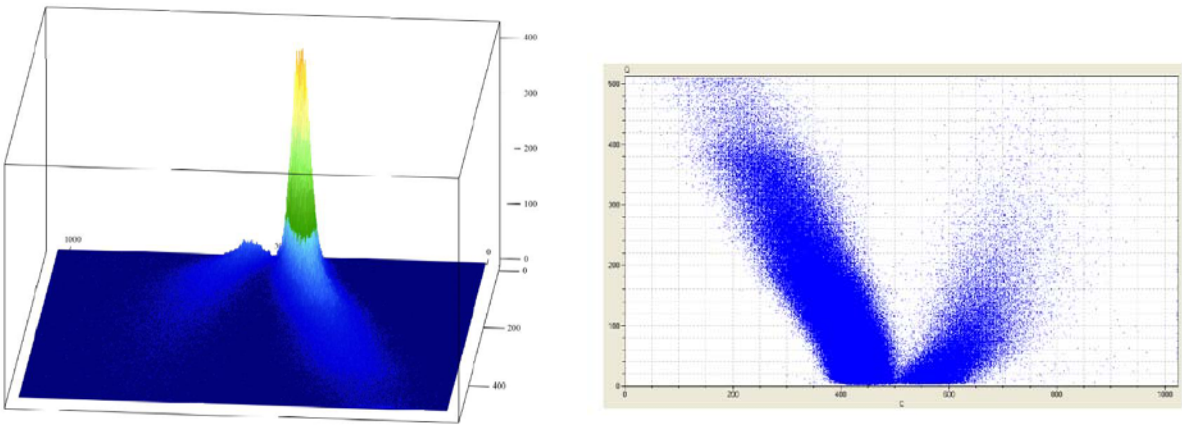

Figure 11: **C** characteristics according to the method from chapter 1.4 for file _data_10000_Dupr.csv

## CONCLUSION

The described models necessary separation proved as easy usable. To implement ones into the digital spectrometer, all models appear to be readily applicable to technical equipment. Digital spectrometer of the project SPECTRUM is equipped with FPGA. Described models can be implemented into the FPGA and thus significantly reducing the width of stream spectrometric system data channel. This ability will be a major contribution to the ON-LINE application.

## LITERATURE


[1] Glenn F. Knoll. Radiation Detection and Measurement, third edition, 2000 John Wiley & Sons, Inc. ISBN-0-47-0738-5.

[2] EJ-444 Dual Phosphor Thin Scintillator, www.eljentechnology.com

[3] T.K. Alexander, F.S. Goulding. An amplitude-insensitive system that distinguishes pulses of different shapes, Nuclear Instruments and Methods, Volume 13, August–October 1961, Pages 244-246, ISSN 0029-554X, 10.1016/0029-554X(61)90198-7.

[4] M.L. Roush, M.A. Wilson, W.F. Hornyak. Pulse shape discrimination, Nuclear Instruments and Methods, Volume 31, Issue 1, 1 December 1964, Pages 112-124, ISSN 0029-554X, 10.1016/0029-554X(64)90333-7.

[6] J.M. Adams, G. White. A versatile pulse shape discriminator for charged particle separation and its application to fast neutron time-of-flight spectroscopy. Nuclear Instruments and Methods, 156(3):459-476, 1978. Sons, Inc. ISBN-0-47-0738-5.

**Acknowledgement**
The work presented in this paper has been supported under the research project SPECTRUM, No. TA01011383 by Technology Agency of the Czech Republic.